

## DESIGN AND TEST OF A 1.3 GHz TRAVELLING WAVE WINDOW

C. Travier<sup>#</sup>, S. Chel, M. Desmons, G. Devanz,

CEA/DSM/DAPNIA, Bat 701, L'Orme des Merisiers, 91191 Gif-sur-Yvette, France,

P. Lepercq, T. Garvey,

LAL/IN2P3/CNRS, Bat 200, BP 34, 91898 Orsay Cedex, France

### Abstract

As part of an R&D program to develop an input power coupler for the TESLA project, a 1.3 GHz travelling wave window was designed, fabricated and tested. The main advantages of this window are a reduced electric field at the brazing location, low dielectric losses and protection of the ceramic from the direct view of the electrons coming from the cavity. Two versions of this window were fabricated (one with titanium as the outer conductor, and one with a copper outer conductor). The titanium version was tested up to 1 MW (1 ms), both at room temperature and at 100 K. The design of this window, and the results of the high power tests are presented in this paper.

### 1 INTRODUCTION

Within the TESLA collaboration R&D effort, the CEA and IN2P3 are involved in a power coupler development program, that was first presented at EPAC96 [1]. The power test stand was presented together with the first experimental results in reference [2], while the test of a very simple  $\lambda/2$  window was reported at the last PAC conference [3]. The present paper concerns the design, fabrication and high power tests of a 1.3 GHz travelling wave (TW) window.

### 2 FRAMEWORK

In a superconducting linear accelerator, input power couplers are one of the key components, to which special attention has to be given in order to ensure guaranteed performances and full reliability. Since the beginning of the TESLA R&D effort through the TTF project, a lot of work has been done on power couplers both at Fermilab [4-6] and DESY [7-10]. However, two strong reasons argue in favor of more endeavor: (1) cost reduction in view of the fact that several thousand couplers are needed for TESLA, and that the prototype couplers are expensive pieces of equipment, (2) performance increase linked to the concept of the superstructure proposed by J. Sekutowicz [11]. These two reasons are driving the R&D effort being made by the French collaboration. It is believed that drastic cost reduction requires work in several directions: simplification of the design, reduction of the number of fabrication steps, simplification of

fabrication procedures. Furthermore the effort should first be devoted to the more expensive and complex elements of the coupler, which are mainly RF windows and waveguide to coax transitions.

Concerning RF windows, it was decided to concentrate on disc type windows, since we believe they present the highest potential for cost reduction, due to their simpler geometry. Two types were designed, fabricated and tested: the  $\lambda/2$  window [3] and the TW window. This paper concentrates on the latter. The first part of the paper presents the design of the TW window. Low level RF measurements compared with SUPERFISH [17] simulations are then given. Before discussing high power tests, both at room and liquid nitrogen temperature, the test stand is described as well as the conditioning procedure.

### 3 DESIGN OF THE TRAVELLING WAVE WINDOW

#### 3.1 Design considerations

The concept of TW window was first proposed by Kasakov [12], and the application to the TESLA coupler was suggested by Hanus and Mosnier [13]. The principle of a TW window is to establish inside the ceramic a pure travelling wave. This is done by a matching inductive or capacitive component located on both sides of the ceramic, so that the impedance of this element loaded by a coaxial line is equal to the impedance of the ceramic. A global matching of the window would lead to some standing wave inside the ceramic and thus to an increased field when compared to the pure travelling wave. For example, in reference [14], it is shown that a TW window allows one to reduce the maximum field inside the ceramic by a factor 4 when compared to a half-wave resonant window, and a factor of 2 versus the maximum field in the waveguide.

For a coaxial type window, the easiest way to achieve a pure travelling wave in the ceramic, is to use a capacitive iris on both side. This approach was followed in reference [13] and also leads to maximum field inside the ceramic a factor of 2 smaller than the field on the inner conductor of the coaxial line. The resulting geometry has however two drawbacks: it is difficult to achieve a practical mechanical assembly and electron or

<sup>#</sup> E-mail: [ctravier@cea.fr](mailto:ctravier@cea.fr)

X-rays coming from the cavity might strike the ceramic. This latter effect proved to be harmful for the CEBAF couplers [15]. Though the geometry is significantly more favorable in the case of a coaxial coupler, when compared to CEBAF waveguide couplers, it is interesting to try to imagine a window that would not allow such direct impact of cavity electrons or X-rays.

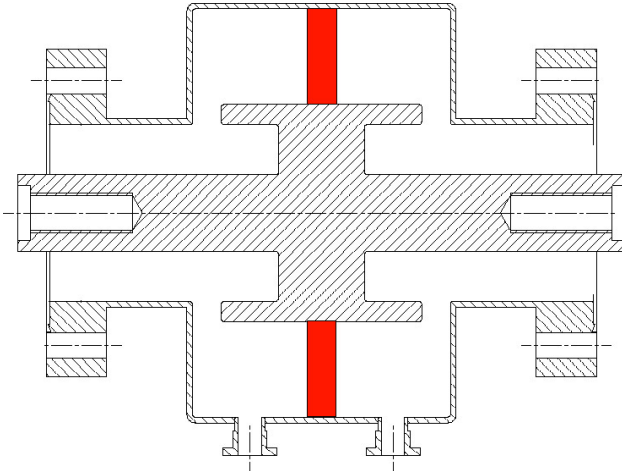


Figure 1: Sketch of the travelling wave window

Reducing the maximum electric field inside the ceramic and at the triple point (ceramic, metal, vacuum), together with shielding the ceramic from cavity electrons and X-rays, lead us to the design of the TW window shown in figure 1. The ceramic is hidden in an outer "cavity", which can be viewed as a piece of coaxial line of larger inner diameter short-circuited and coupled to the main coaxial line through coupling gaps. The larger inner diameter allows us to obtain a maximum field at the triple point and inside the ceramic which is only 25% of the maximum field on the inner conductor of the 61.8 mm diameter coaxial line.

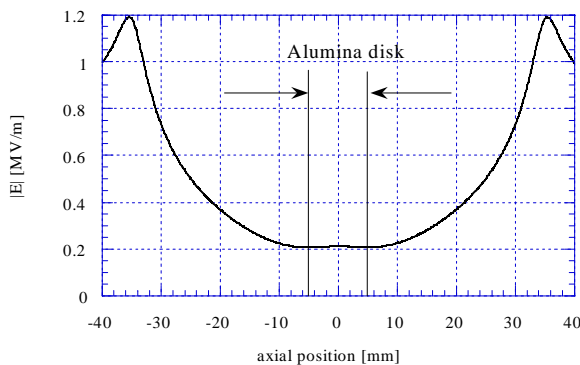


Figure 2: Electric field envelope in the ceramic disk region for 1 MW incident power

Figure 2 shows the flat field envelope inside the ceramic, which is a distinctive mark of a TW window. The maximum field inside the window is reached on the

"nose" of the coupling gap and its value is 2 times the field on the inner coax conductor.

### 3.2 Mechanical design

The window was fabricated in the following way: the ceramic was first brazed to an inner and outer collar. The collars were then welded to the remaining parts of the conductors. Two different materials were used to fabricate the outer conductor: titanium and copper. In both cases, the inner conductor was made of copper. The two windows, referred thereafter as the "titanium" and "copper" windows were fabricated by SICN [16]. Wesgo Al300 alumina (97.5 % purity) was used. The brazing was done in such a way that braze material didn't leak onto the ceramic or the conductor. Both faces of the ceramic were coated before brazing with a thin layer of TiN (target value 5 nm) deposited by magnetron sputtering.

## 4 LOW LEVEL RF MEASUREMENTS

Figure 3 shows the measured and simulated  $S_{11}$  curve around the operating frequency for the two windows. Figure 4 shows the high frequency part of the curve (up to 7 GHz), for the titanium window. The bandwidth corresponding to a VSWR of  $-20$  dB is 60 MHz.

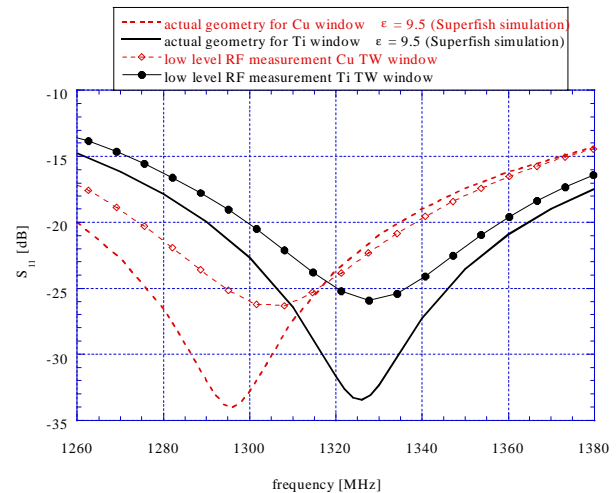


Figure 3: Measured and simulated  $S_{11}$  curve around 1.3 GHz.

The simulations are done with SUPERFISH [17], using a mesh size of 0.5 mm. The measured curve is well reproduced (as far as the minimum SWR is concerned) when rounded edges necessary, for mechanical fabrication, real dimensions obtained from measurements and true dielectric constant of the ceramic are used. This dielectric constant value ( $\epsilon = 9.5$ , to be compared to the value given by the vendor  $\epsilon = 9$ ) is deduced from the measurement of the minimum SWR obtained for a half-wavelength disk window made of the same ceramic.

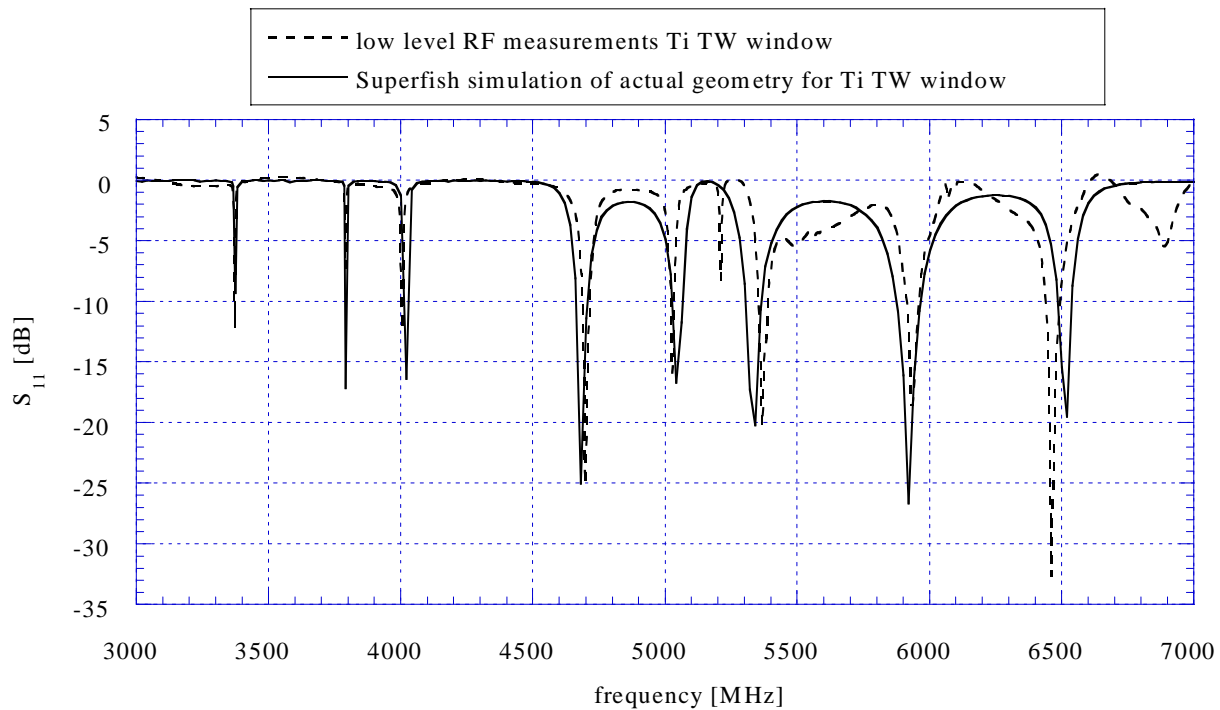


Figure 4: Comparison between the measured and simulated  $S_{11}$  curve of the titanium window between 3 and 7 GHz

The agreement is somewhat poorer for the copper window: we believe that this comes from the fact that the dimensions were measured manually in this case, whereas the dimensions of the titanium window were measured with a 3D machine

## 5 HIGH POWER TESTS OF THE "TITANIUM WINDOW"

### 5.1 The test stand

The power stand has already been described in references [1] and [2]. It consists of a power source (THOMSON klystron TH2086A) feeding a long waveguide as shown schematically in figure 5. The coaxial components to test (window, tapered line, bellow, ...) are inserted between two waveguide to coax transitions. If one of these transitions is an antenna type transition, it is possible to test an entire coupler. This stand has two operational modes:

- when the waveguide is short-circuited, a standing-wave pattern is established, which means that each element sees a different value of the electric field. By varying the frequency, it is possible to move the position of the nodes of the electric field along the line, and therefore test the elements under all field values. According to the length of the waveguide (around 5 m), the necessary frequency span to have a complete field variation at the position of the element under test is around 40 MHz.

- when the waveguide is terminated with a matched load, a pure travelling wave exists in the system and all elements see the same electric field that is, for a given input power, 4 times less than the maximum field in the standing wave case.

The modulator is simply made of a big capacitor, so that the repetition rate is limited to 0.1 Hz. The high voltage produced by the discharge of this capacitor is naturally not flat. In order to have a flat top RF pulse, one has therefore to control the shape of the RF drive pulse, which is done by a feedback loop. The klystron itself can deliver more than 1 MW, but in the present configuration, the maximum available power (for a flat top pulse) depends on the frequency and pulse duration. At 1300 MHz, one can reach 1.7 MW for 0.5 ms and only 1 MW for 1 ms.

The waveguide between the exit of the klystron and a THOMSON TH20141A window is at atmospheric pressure. Between this window and the short or another window in front of the load, the waveguide is under vacuum. The vacuum is obtained through two ion pumps (150 l/s) located on each side of the travelling wave window. The vacuum levels are directly read from the pump currents and used as a diagnostic tool. The value of the vacuum level just before the RF pulse and the maximum value reached after the RF pulse are recorded on a log file for each RF pulse.

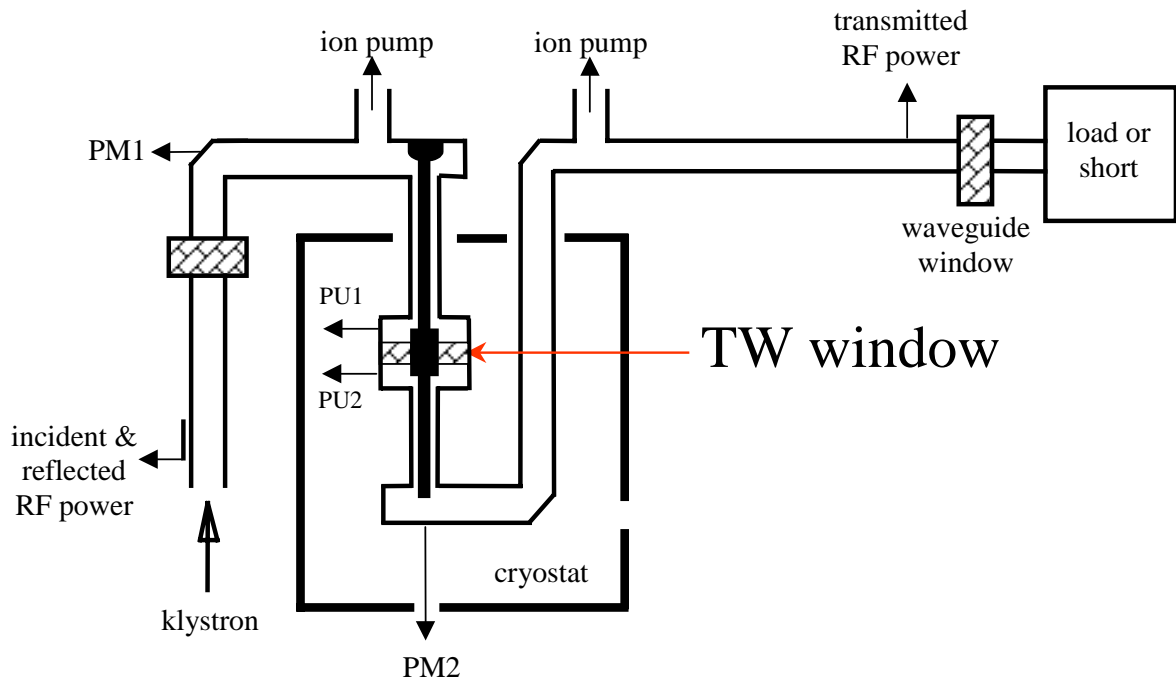


Figure 5: Schematic of test stand showing instrumentation

In order to test the coupler in a more realistic environment, a liquid nitrogen cryostat was built [2]. It allows one to maintain the window under test at around 100K thus roughly reproducing what is happening in the TESLA coupler. This situation allows us to test the mechanical behavior of the window, to measure thermal losses and to check if RF conditioning at cold temperature is or is not different from that at room temperature. A photograph of the inside view of the cryostat, showing the

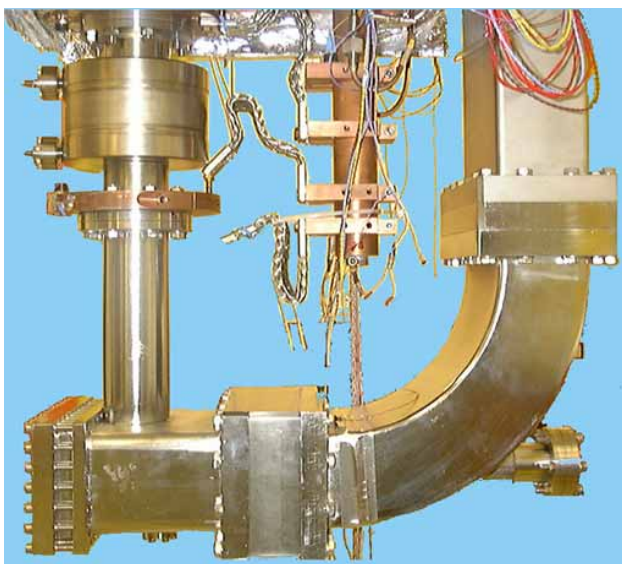


Figure 6: View of the window and coax to waveguide transition.

titanium window, the antenna waveguide to coax transition and the "cold box" is given on figure 6.

The test stand is equipped with RF and electron pick-ups to measure simultaneously the electric field and the electron current, and with photomultipliers (PM) to record the light produced during the RF pulses. The precise location of these diagnostics is indicated in figure 5. The electron pick-ups are polarized with a positive voltage of 50 V. The PM and electron signals, together with RF signals coming out of the detection diodes, are sampled at 100 kHz.

The test stand is fully computerized, through a personal computer running a LABVIEW application. Digitized signals and signal history are displayed on the LABVIEW screen. Altogether, around 70 parameters are stored for each pulse (this number can vary slightly depending on the test being done) for off-line processing and analysis. This storage produces around 12 Mo of data per day. For a typical coupler experiment as presented in this paper, one has between 50,000 and 500,000 pulses, i.e. between 60 and 600 Mo of data. For the analysis of the experiment, it is important to access all these data at the same time, in order to be able to make cross correlation and try to explain the origin of phenomena. Due to this huge amount of data, we found that the most suitable post processor software is PAW [18] which was developed at CERN for high energy physics experiments. A Fortran program calling the HBOOK [19] library is first used to fill the "ntuples" which are then analyzed with PAW. At this stage the data using binary encoding, needs around 30 Mo of disk space per 100,000 pulses.

## 5.2 Conditioning

Prior to mechanical assembly, all the pieces including the window were baked at 300°C for 4 hours in a vacuum furnace. After assembly and leak test, the window and neighboring elements (such as waveguide to coax transitions, ions pumps, coaxial conductors and waveguides) were baked in-situ up to 120°C for one week. Calibration of thermal responses of temperature probes were conducted for a week. Such a long time is necessary because the thermal equilibrium can only be reached after more than 12 hours. Since the RF conditioning started three weeks after the vacuum sealing, and two weeks after the end of the baking, the initial vacuum on both sides of the window was  $5 \cdot 10^{-8}$  mbar. Due to a leak in a valve on the cryogenic system, a flow of liquid nitrogen was continuously cooling the window, so that while RF conditioning (under TW), the window was at 220 K.

The conditioning procedure is established as follows: a RF power pulse of 0.8 ms is applied to the window. If electron, or PM or vacuum signals are higher than given thresholds, the power is switched off by hardware interlocks. These thresholds are chosen as follows: electron threshold: 5 mA, PM threshold: approximately  $10^8$  photons, vacuum threshold called  $V_{interlock}$ :  $10^{-5}$  mbar. Electron and PM interlocks are fast (5  $\mu$ s) and can switch the power during the pulse. Vacuum interlocks can only react on the following pulse. In order to speed up the conditioning process, and owing to the fact that our repetition rate is very low, it was decided not to wait for the next pulse to switch back on the RF power, in the case it was switched off by one of the fast interlocks. Power is switched back on after a 50  $\mu$ s delay. In the case of very fast rise time of electron or PM signals, one can have as much as 10 successive micropulses, within a normal 0.8 ms pulse.

In order to allow the increase of power, one has to fulfill two conditions : for two consecutive pulses, the outgassing during the pulse should be less than a limit  $V_{limit}$  chosen by the operator (usually  $10^{-7}$  mbar), and the power should not be switched off by the fast interlock. If these conditions are fulfilled, a power increment of 10 kW is applied. If the vacuum outgassing is larger than  $V_{limit}$ , but the vacuum level is lower than  $V_{interlock}$ , the power is kept constant. If it is higher than  $V_{interlock}$ , the power is decreased by 10 kW. When the power reaches the maximum power range allowed by the operator, the ramping is started again from the beginning. After a while, the authorized maximum power range is increased. The following maximum power ranges were used in the present case: 200, 500, 800 and 1000 kW. The maximum power of 1 MW was reached after 21,000 pulses, which corresponds to 58 hours and is equivalent to 35 minutes at 10 Hz operation. Figure 7 shows the power ramping achieved for the first conditioning of the window (The pulses 7,500 to 10,000 were used to obtain the SWR of the system in the whole possible frequency range). After

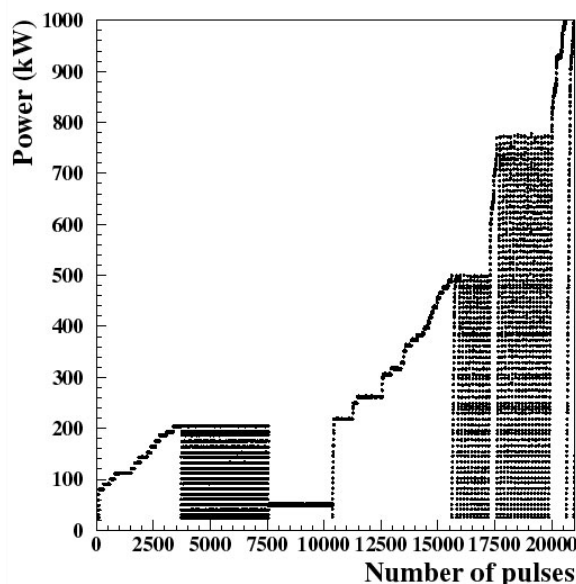


Figure 7: First conditioning of the window up to 1 MW incident power

this first conditioning, the window was operated 24 hours a day for almost three months, according to the sequence described in table 1, accumulating 483,000 pulses.

Table 1: Operating sequence of TW "titanium" window

| Number of pulses          | Power level (kW) | Temperature (K) | Comment            |
|---------------------------|------------------|-----------------|--------------------|
| Travelling wave operation |                  |                 |                    |
| 25,500                    | 0-1000           | 230             | conditioning       |
| 1,700                     | 0-400            | 250             |                    |
| 8,800                     | 400-650          | 250             |                    |
| 25,000                    | 300-1000         | 250             |                    |
| 26,600                    | 500-1000         | 250             |                    |
| Standing wave operation   |                  |                 |                    |
| 44,400                    | 0-1000           | 230             |                    |
| 8,000                     | 0-1000           | 230 → 105       | cooling            |
| 7,000                     | 1000             | 105             |                    |
| 26,000                    | 0-1000           | 105             |                    |
| 12,000                    | 1000             | 105             |                    |
| Travelling wave operation |                  |                 |                    |
| 15,000                    | 0-1000           | 105             |                    |
| 4,000                     | 100              | 175             | Window baking      |
| 21,000                    | 0-1000           | 105             |                    |
| 9,000                     | 1000             | 105             | Losses measurement |
| 13,000                    | 0-1000           | 105             |                    |
| 27,000                    | 0-1000           | 250             |                    |
| 18,000                    | 1000             | 250 → 300       |                    |
| 42,000                    | 0-1000           | 300             |                    |
| 33,000                    | 500-1000         | 105             |                    |
| 74,000                    | 0-1000           | 300             |                    |
| 8,000                     | 1000             | 300             |                    |
| 28,000                    | 700-800          | 300             |                    |
| 9,000                     | 1000             | 300             |                    |

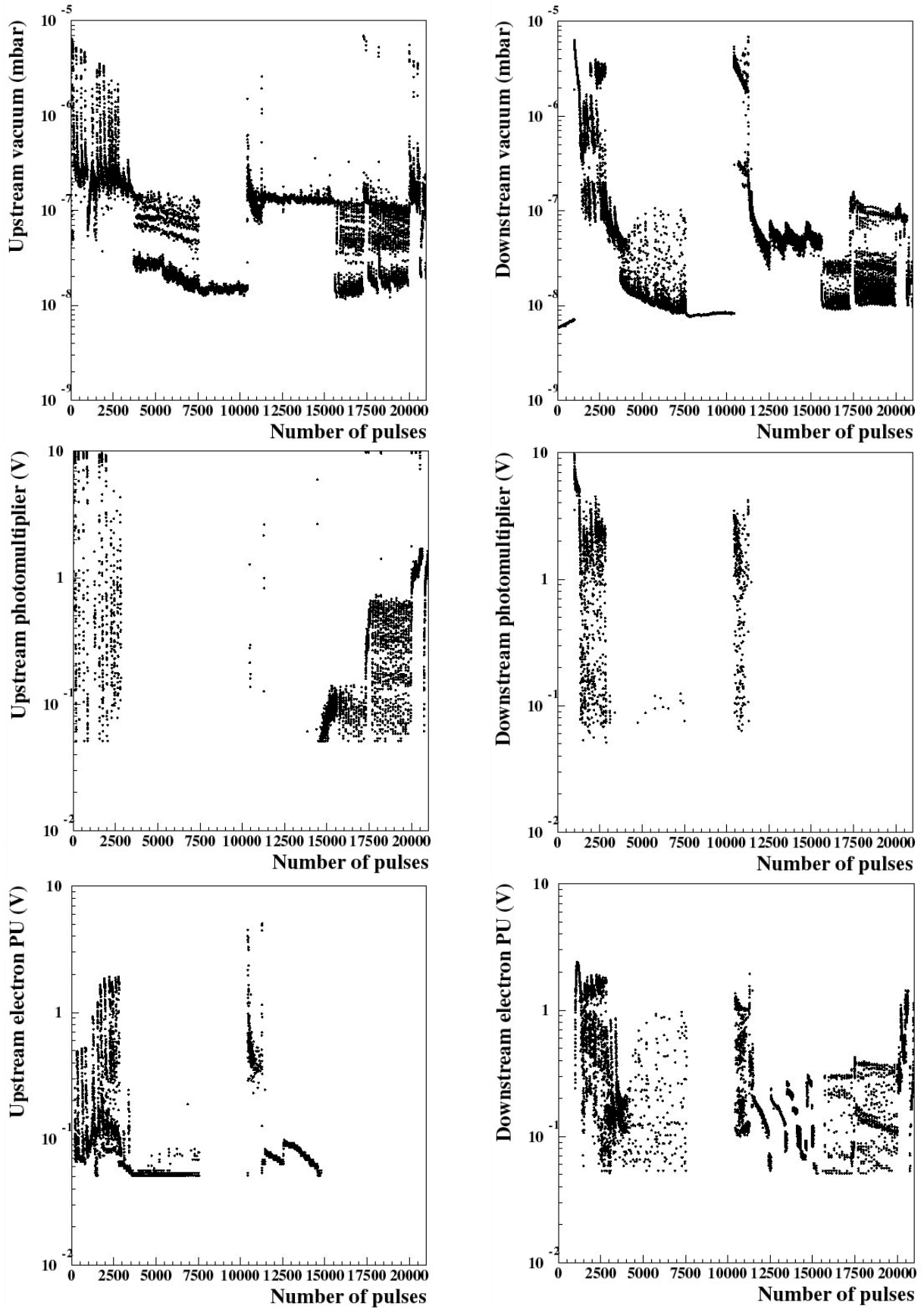


Figure 8 : Vacuum, photomultiplier and electron signals during the first conditioning. Upstream signals are on the left, downstream on the right.

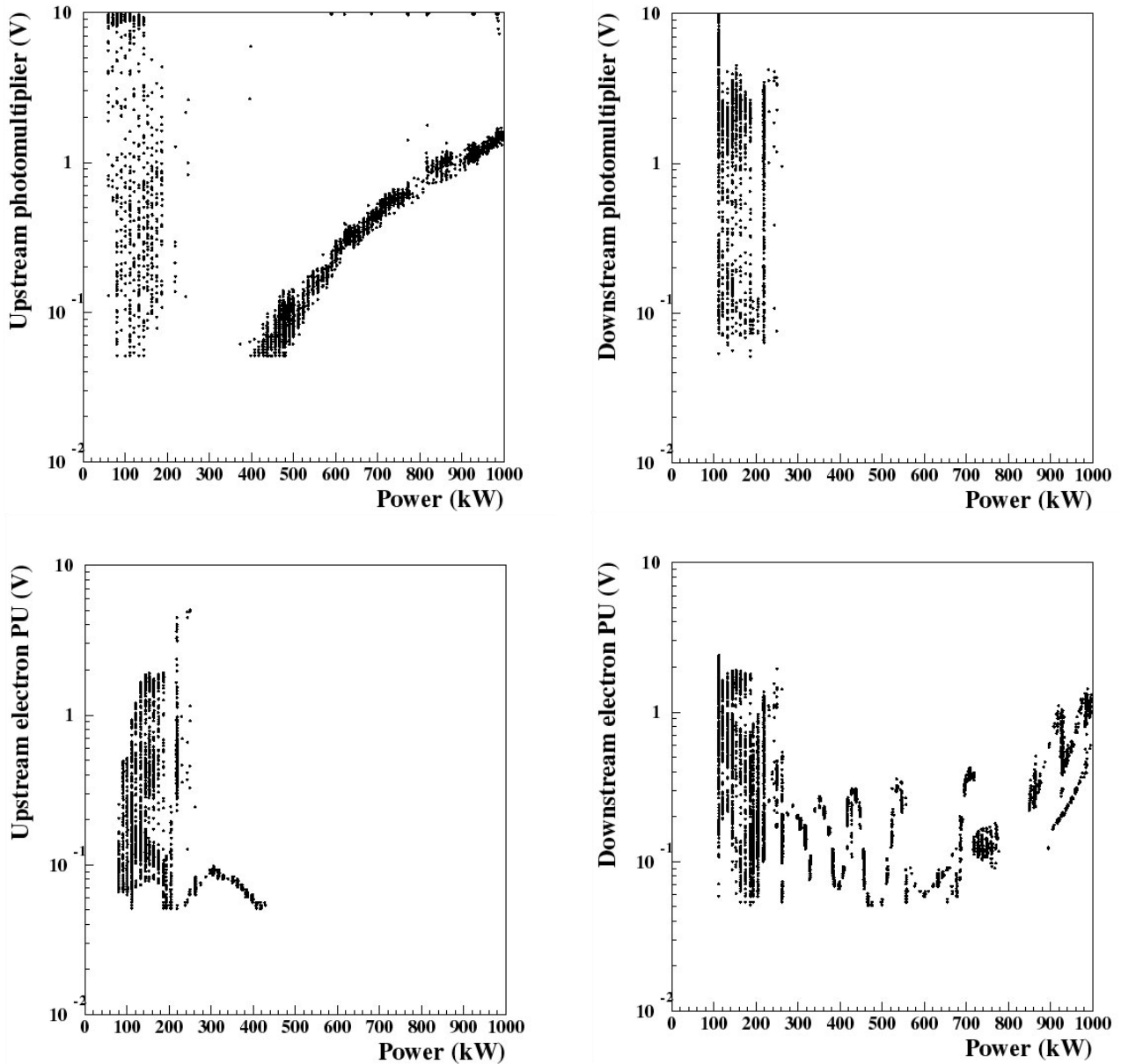


Figure 9 : Photomultiplier and electron signals during the first conditioning as a function of incident RF power.

### 5.3 Analysis of conditioning period

We first present the results obtained during the first power ramping which lasted for 21,000 pulses. Figure 8 shows electron, light signals and vacuum outgassing, as a function of the number of pulses. The same signals are shown as a function of input power on figure 9. The following remarks are worth noting:

- All signals are intense at low power (below 200 kW), but the corresponding phenomena are rapidly processed. Since they are seen by all detectors, they are most likely related to the coaxial line. They probably correspond to weak multipactor barriers, but also to small arcing and field emission associated

with the normal processing of a new component exposed to RF.

- The light detected by the upper PM looking towards the doorknob waveguide to coax transition, increases smoothly with the power for values larger than 400 kW. This phenomenon has already been observed in previous experiments, and is the signature of something happening in the doorknob transition, between the short-circuit and the doorknob. Very large signals (10 V) indicate a saturation of the PM associated with a spark inside the transition. A detailed analysis of the signal in this power range reveals the presence of another phenomenon that produces a much smaller signal, as will be explained in the following subsection.

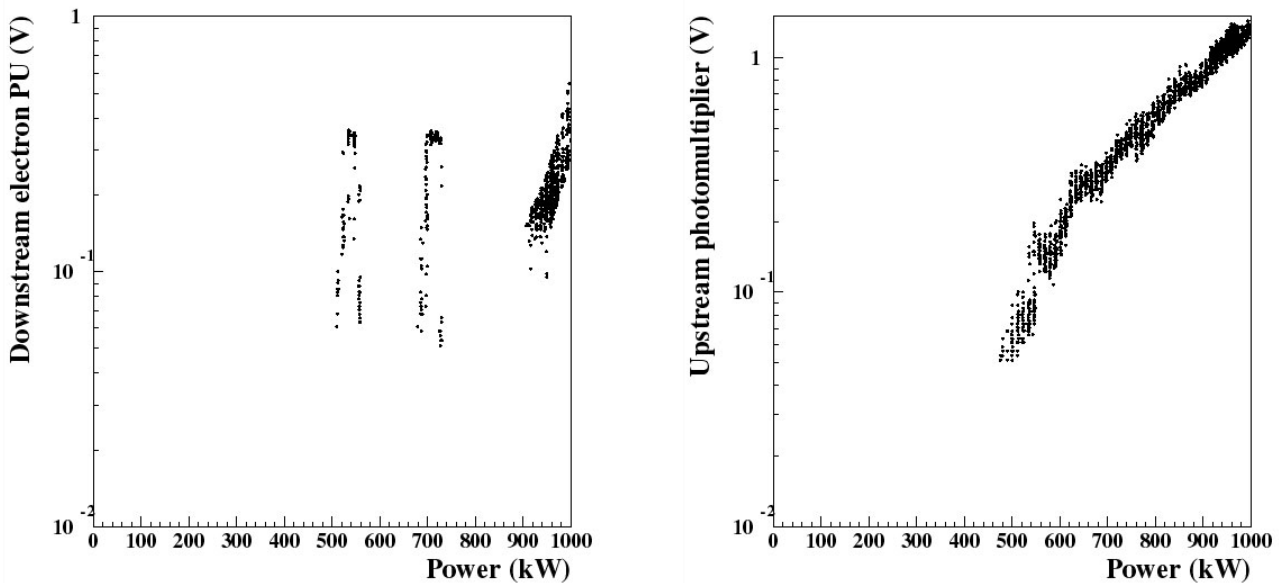


Figure 10 : Downstream electron and upstream PM signals during the first power cycling.

- The upstream electron pick-up reveals a small (< 100 mV) signal between 200 and 400 kW. This signal is only 100  $\mu$ s long, as opposed to the signal between 0 and 200 kW which lasts between 500 and 800  $\mu$ s. This non-zero electron signal is obtained during the first ramping between 200 and 400 kW, corresponding to pulses 11,000 to 15,000 as shown in figure 7. The interpretation of this signal which is not seen on other diagnostics is difficult. Moreover, it was found later on, that one of the cable connecting this pick-up to its amplifier was defective.
- On the downstream side of the window, the electron pick-up signal exhibits several barriers. Many of them are quickly processed away as will be shown in the following subsection. These signals could come from the window cavity and/or the coaxial line.

Table 2 : Barriers found during power ramping

| Barriers found on vacuum signals (kW) | Barriers found on PM signals (kW) |
|---------------------------------------|-----------------------------------|
| 435                                   | 410                               |
| 490                                   | 515                               |
| 555                                   | 555                               |
| 585                                   | -                                 |
| 645                                   | 635                               |
| 705                                   | 715                               |
| 745                                   | 745                               |
| 860                                   | 860                               |
| 940                                   | 960                               |
| 1005                                  | 990                               |

Knowing that the power ramping steps are 10 kW and owing to the fact that the signals are very small, the two sets of barrier levels are in a reasonable agreement. The most probable interpretation of these measurements is that the smoothly varying PM signal corresponding to very small outgassing comes from the doorknob transition, where the multipacting barriers are those of the coaxial line and/or the bellows present in this line.

### 5.4 First power cycling

Once the power has reached 1 MW, repetitive power ramping between 0 and 1 MW is done. Figure 10 presents the results corresponding to the first sets of these power ramps, between pulse 21,000 and 25,000. The downstream light detector does not produce any signals. The upstream PM still shows the behavior described earlier, typical of the doorknob transition, while on the downstream pick-up signals, only 3 barriers remain (550, 700 and 1000 kW), which are also present on the vacuum outgassing, not shown here. A close look to the upstream PM signal reveals discrete barriers superimposed on a smoothly increasing signal. These barriers are clearly seen on figure 11 where the smoothly increasing signal obtained by a parabolic fit has been subtracted from the PM signal, that has then been averaged. Figure 12 shows the same barriers on the vacuum outgassing. Table 2 summarizes the barriers found on the 2 signals.

### 5.5 Steady state operation

After the conditioning period and the first few power ramps, the test stand was operated in the standing wave mode. The results are not presented here as, due to a poor matching of the system, the standing wave operation was quite difficult to analyze. However, its main result was to fully process the doorknob transition, so that the smoothly varying PM signal barely disappeared when going back to the travelling wave operation. The window was then operated again in the travelling wave regime for

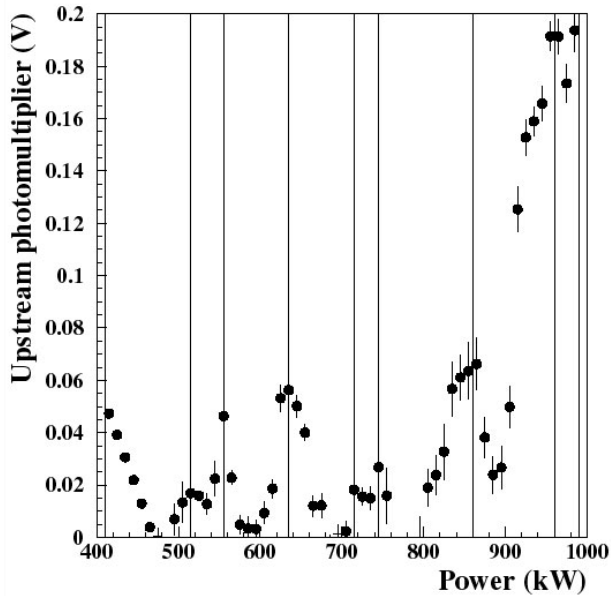


Figure 11 : Upstream PM signal with smoothly varying component subtracted, showing multipactor barriers.

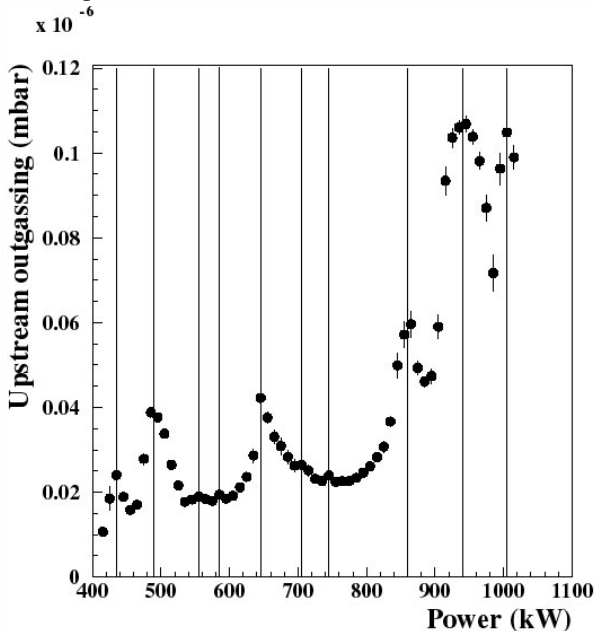


Figure 12 : Upstream outgassing signal, showing multipactor barriers.

more than 200,000 pulses, both at room temperature and at 100 K. The results for these two conditions are basically the same, except for the outgassing which is slightly higher at room temperature.

At the end, when the window is fully conditioned, one can hardly detect any signals:

- The upstream PM shows a very weak signal ( $< 200$  mV) between 600 and 1000 kW as shown in figure 13. The coaxial line multipacting barriers recorded in table 2 disappear progressively. The last ones to be seen clearly are 650, 700 and 750 kW. When the signal is below 200 mV, these barriers merge into a

single one, at the level of the detector sensitivity. The very small signal above 900 kW is the remaining sign of the smoothly increasing signal from the doorknob transition.

- The electron pick-ups and the downstream PM do not detect any signals. On the downstream side, the vacuum outgassing as a function of the power reveals the same multipactor barrier at 700 kW already observed during the conditioning (figure 10). This barrier, corresponding to multipactor inside the coax line, is the hardest to process. However the level of outgassing is so small ( $3-4 \cdot 10^{-9}$  mbar) that it is not harmful.

Due to the low duty cycle ( $6 \cdot 10^{-5}$ ), the calculated dielectric losses at 1 MW (assuming  $\tan\delta = 3 \cdot 10^{-4}$ ) are only 20 mW. They are much less than the losses in the titanium and stainless steel conductors, and it was therefore not possible to measure them.

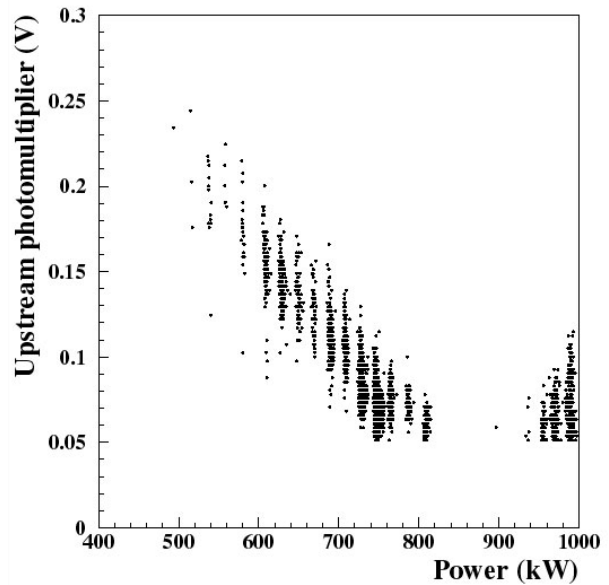


Figure 13: Upstream PM signal at the end of the test

## 6 CONCLUSION

The window presented in this paper is one of the first (if not the first) coaxial TW window. It was shown that this window could be rapidly processed. It was then successfully operated for several months, both at room temperature and at 100 K, at a power level up to 1 MW (limited by RF source). The window did not exhibit any strong multipacting barriers during the conditioning period and no multipacting at all after conditioning. The copper version of the window will be tested in the near future.

## 7 ACKNOWLEDGEMENTS

We would like to thank all the people at IN2P3 and DAPNIA involved in this work for the design, construction and operation of the test stand. A special thanks to A. Hamdi who performed the low level measurements presented in this paper. M. Durand from SICN company should be credited with the mechanical design and fabrication of the windows.

## 8 REFERENCES

- [1] Chel S. et al., "Power coupler development for superconducting cavities", Proceedings of the Fifth EPAC, June 10-14, 1996, Sitges, pp. 2088-2090.
- [2] Chel S. et al., "Status of the TESLA power coupler development programme in France", Proceedings of the Sixth EPAC, June 22-26, 1998, Stockholm, pp. 1882-1884.
- [3] Chel S. et al., "Coaxial disc window for a high power superconducting cavity input coupler", Proceedings of the 1999 PAC, March 29-April 2, 1999, New-York, pp. 916-918.
- [4] M. Champion, "TESLA input coupler development", Proceedings of the 1993 PAC, May 17-20, 1993, Washington, pp. 809-811.
- [5] D. Sun et al., "High power test of RF window and coaxial line in vacuum", Proceedings of the 1993 PAC, May 17-20, 1993, Washington, pp. 30-32.
- [6] M. Champion, "Design, performance and production of the Fermilab TESLA RF input coupler", Proceedings of the 1996 Linear Accelerator Conference, August 26-30, 1996, Geneva, CERN 96-07, pp. 521-523.
- [7] B. Dwersteg et al., "Conceptual Design of a RF Input Coupler for TESLA", Proceedings of the HEACC 92, July 20-24, 1992, Hamburg, pp. 954-956.
- [8] B. Dwersteg et al., "TESLA main coupler development at DESY", Proceedings of the 6th Workshop on RF superconductivity, October 4-8, 1993, Newport News, pp. 1144-1150.
- [9] B. Dwersteg, "High Power Windows at DESY, Operation Experiences, Development Work on TTF Input Couplers", Proceedings of the 8th Workshop on RF superconductivity, October 6-10, 1997, Abano Terme, pp. 740-752.
- [10] W.D. Moeller, "High-Power Coupler for TESLA Test Facility", Proceedings of the 9th Workshop on RF superconductivity, November 1-5, 1999, Santa Fe.
- [11] Sekutowicz J., Ferrario M., Tang C., "Superconducting superstructure for the TESLA collider: a concept", Phys. Rev. Special Topics - Accelerators and Beams, Vol. 2, 062001 (1999).
- [12] Yu. Kasakov, "Increased Power RF-Windows", BINP Preprint 92-2, Protvino, 1992.
- [13] X. Hanus, A. Mosnier, "Coaxial TW window for power couplers and multipactor considerations", Proceedings of the 7th Workshop on RF Superconductivity, Oct. 17-20, Gif-sur-Yvette, 1995, pp. 701-705.
- [14] W.R. Fowkes et al., "Reduced field TE01 X-band travelling wave window", Proceedings of the 1995 PAC, May 1-5, 1995, Dallas, pp. 1587-1589.
- [15] T. Powers, P. Kneisel, "Arcing Phenomena on CEBAF RF-Windows at Cryogenic Temperatures", Proceedings of the 7th Workshop on RF superconductivity, Oct. 17-20, Gif-sur-Yvette, 1995, pp.713-717.
- [16] SICN, BP 1, 38113, Veurey-Voroize, France.
- [17] Poisson-Superfish, J. H. Billen, L. M. Young, LA-UR-96-1834, 1998.
- [18] PAW, CERN Program Library Long Writeup Q 121, 1995.
- [19] HBOOK, Reference manual, Version 4.22, Application software group, Computing and networking division, CERN, 1994.